

Distinguishing between a true period and its alias, and other tasks of model discrimination

Roman V. Baluev*

*Central (Pulkovo) Astronomical Observatory of Russian Academy of Sciences, Pulkovskoe sh. 65/1, St Petersburg 196140, Russia
Sobolev Astronomical Institute, St Petersburg State University, Universitetskij prospekt 28, Petrodvorets, St Petersburg 198504, Russia*

Accepted 2012 February 21. in original form 2011 May 31

ABSTRACT

We consider the task of distinguishing between two different alternative models that can roughly equally explain observed time series data, mainly focusing on the period ambiguity case (aliasing). We propose a test for checking whether the rival models are observationally equivalent for now or they are already distinguishable. It is the Vuong closeness test, which is based on the Kullback-Leibler Information Criterion. It is asymptotically normal and can work (in certain sense) even in the misspecified case, when the both proposed alternatives are actually wrong. This test is also very simple for practical use. We apply it to several known extrasolar planetary systems and find that our method often helps to resolve various model ambiguities emerging in astronomical practice, but preventing us from hasty conclusions in other cases.

Key words: methods: data analysis - methods: statistical - surveys

1 INTRODUCTION

The search for periodicities is one of the most basic tasks of the observational data analysis. This task emerges in all or almost all branches of astronomy (and even not only astronomy), which deal with observational (or experimental) data. This task is usually solved by means of the periodogram-based approach. In this approach, one considers certain function of a period (or frequency), which basically represents some estimation of the power spectrum of the observed process. Such estimating function is traditionally called a *periodogram*, and there are many types of periodograms that are used in practice. The Lomb (1976) – Scargle (1982) periodogram is a popular choice, for instance.

The observed data are usually noisy and, consequently, such data produce noisy periodograms. This implies that some statistical issues should be usually resolved during the period search procedure. The first such issue is the determination of the statistical significance of the extracted periodicities. This problem is already investigated in advance by various authors, see e.g. (Frescura et al. 2008) and (Baluev 2008) for a recent review.

The present work is devoted to another issue, which arises when the original data are not spaced uniformly in time. In astronomy, it is a frequent case when the observations are gapped in time due to several natural phenomena like the day/night cycle, moonlight contamination, etc. It is well-known that such data produce so-called *aliases*,

that is false stroboscopic periods contaminating the periodograms. Sometimes, it is even difficult to say, which periodogram peak is the real one and which is its alias. Our paper will focus on this situation of the alias ambiguity. The periodograms themselves are usually easily calculated using pretty simple formulae. Recent results (Baluev 2008) also allow very simple (but rigorously justified) assessing of the significance of the extracted periods. However, there is a lack of similarly simple and rigorous methods solving the alias discrimination task.

In a particular application, we usually have, in addition to the raw time series data, some prior information concerning the phenomenon under research. This information often can be used to select one of the available alternatives, or at least to retract some of them, making the final pool of solutions more narrow. For example, in the exoplanet radial velocity searches, a popular approach involves various dynamical stability or regularity criteria (Goździewski et al. 2006; Goździewski et al. 2007; Goździewski et al. 2008). No doubt, such methods are useful, but we would often prefer not to bind ourselves to any external assumptions as much as possible, allowing the data to speak for themselves. For example, in the case of exoplanet searches, the apparent radial velocity patterns can often be caused by stellar activity effects rather than by orbiting planets. In such a case any dynamical criteria may be unreliable, since we cannot be sure even that a given radial velocity oscillation is indeed induced by a really existing planet.

In other words, in this work we put a goal to find a purely statistical method of alias discrimination, that could

* E-mail: roman@astro.spbu.ru

be maximally independent on various prior assumptions. We may highlight a recent work by Dawson & Fabrycky (2010), where the authors propose to take into account the phases of candidate aliases, when choosing between them. However, this approach is not very rigorous, because it basically does not take into account any possible noisy fluctuations of these phases, as well as of the aliases amplitudes. In addition, this approach is not easy to apply in an automated way, since it requires an active participation of the researcher.

The source of the lesser attention to this problem probably comes from the fact that to distinguish aliases we need to compare two *non-nested* models of the data, while most of the traditionally used statistical criteria are usually designed to choose between *nested* models. For example, the signal detection task requires to test some “base” model against a more general “base+signal” model, which includes the original base model as a partial case. The alias ambiguity does not infer nested models: none of the two alternative periodicities can encompass another one as a partial case. Such situation usually falls out of a typical handbook on mathematical statistics. Nevertheless, we find that there are many individual statistical works dealing with tests for non-nested hypotheses, so this statistical problem appears well-studied. Our goal in this paper is to apply these results to the astronomical task of resolving the alias ambiguity, and to construct the appropriate period distinguishing criteria.

The problem is also complicated because we often do not have an accurate model of the real periodic variation. In practice, both alternative models (e.g. simple sinusoids) may be only approximate, and our analysis cannot base on an assumption that one of them is strictly true. Therefore, the method of the analysis should remain valid in the so-called misspecified case, when none of the available models can mimic the true signal precisely, but we are still interested to find out which alternative is better.

The plan of the paper is as follows. In Section 2, we provide a more clear formulation of the problem, what we actually want to derive from our analysis. In Section 3, we describe the basic formulae and ideas of the Vuong statistical test, suitable for solving our task. In Section 4, we provide the final practical formulae of this test. In Section 5, we assess its reliability and efficiency by means of numerical Monte Carlo simulations. Finally, in Section 6, we apply our methods to the analysis of the radial velocity data of several extrasolar planetary system, which demonstrate various alias ambiguities concerning the planetary periods or other model parameters.

2 FORMULATION OF THE PROBLEM

From the first view point, the task can be easily formulated. Assume we have two main peaks in the periodograms, having similar height. We have already established that the periodic signal is significant indeed (at least the larger peak or both peaks are significant), and our first naive question is: which peak we ought to recognise as the true one and which should be accused as its alias? A naive question has a naive answer: we should adopt the taller peak as a more likely candidate. Then the second question arises: how we can ensure that such choice is statistically justified? In other words, is the observed difference between the two peaks statistically

significant? If it is not then any attempt to choose between the two models is, in fact, no better than dropping a coin. In such situation, we can occasionally choose the true period, but such luck cannot be classified as a success of the analysis, since we cannot ensure that we were so lucky indeed. Therefore, we should make available a *third*, inconclusive, outcome of the analysis. This makes the problem qualitatively more complicated, because more types of decisions infer more freedom for making mistakes.

In the framework of the symmetric hypotheses testing with no inconclusive decisions, we have only two possible outcomes, and basically there is only one type of mistakes: accepting a wrong model. In practice, the two models are often treated unequally, however. For example, the first one may be considered as more reliable, while the second one is admitted only hypothetically. In that case we have *two* formal types of mistakes, but the mistakes to wrongly reject the base model are naturally considered as more dangerous. Thus, when applying the traditional statistical tests we first limit the probability of this more dangerous “false alarm”, and only then we try to minimize the mistakes of the second kind, if it is possible. The two types of mistakes are antagonistic: suppressing the frequency of false alarms leads to increased fraction of wrong non-rejections of the null hypothesis.

With *three* decisions at disposal, the following types of mistakes threaten: (I) choosing wrong model when another one is actually better, (II) not choosing any model when one is actually better, and (III) choosing a model when objectively none is really better. The class (I) formally contains two subclasses: to wrongly accept the first or the second model. We consider a symmetric case here, when none of the alternative models is a priori preferable, so these two subclasses are qualitatively equivalent to each other and can be united into one. The three remaining types of mistakes are already qualitatively different. We cannot simultaneously suppress mistakes of all three types, and we cannot say which one is most dangerous in general. It depends on the current practical circumstances: sometimes we cannot tolerate a misclassification, or sometimes an inconclusive answer is highly undesirable. The methods of our paper are designed to suppress the “pink-vision” mistake (III), i.e. the cases when we wrongly assume that the two rival models are distinguishable on the basis of the available observations. The main arguments supporting this choice are:

(i) Such approach allows for an intuitive formalisation of the “statistically justified” choice. We choose any of the alternatives only after we have ensured that they are not observationally equal. Otherwise, we acknowledge that any choice would be too risky for now, and we should live with such ambiguity until more observations resolve it.

(ii) Frequently, none of the proposed models may be correct, and a more accurate model should be constructed to replace both. This task usually cannot be fulfilled reliably until we are ensured that the two original models can be distinguished. It is usually more justified to seek for any theory update only after we managed all its current ambiguities.

(iii) Consider the mutual interaction between the three possible types of the mistakes. For example, suppressing (III), i.e. generating more inconclusive answers, will likely suppress (I) and favours to (II), while suppressing (II) ob-

viously favours to both (I) and (III). In other words, (II) is antagonistic to (I) and (III), while (I) and (III) are not mutually antagonistic. Thus it should be technically convenient to first suppress (I) or (III), which should be broadly equivalent.

(iv) Putting the third-type mistakes in the first place allows us to easily reformulate the problem in the classical hypothesis testing framework, operating in the traditional terms (to a certain point). Indeed, our main task is now to test the null hypothesis “the observed divergence between the two models is consistent with random noise” against the alternative “this divergence is beyond the random noise level”.

We still need to formalise the notion of “observational equivalence” of the rival models. The problem is complicated by the absence of any guarantee that at least one of the alternative models is indeed correct. In true, the signal may have a non-sinusoidal shape (while, e.g., the Lomb-Scargle periodogram implicitly assumes that it is always sinusoidal), and the data may contain some extra small periodic or non-periodic variations. We usually want to know, which model fits the observations *better*, rather than which one is *true*. Therefore, our test should not rely on an assumption that one of the proposed models is correct.

We find that the Vuong test (Vuong 1989) suits our needs very well. This method utilises the Kullback-Leibler Information Criterion (KLIC) to define which of the rival models is “better”.

3 FUNDAMENTALS OF THE TEST

Let us consider two rival models of the data, $\mu_1(t, \boldsymbol{\theta}_1)$ and $\mu_2(t, \boldsymbol{\theta}_2)$ parametrised by the vectorial arguments $\boldsymbol{\theta}_1$ and $\boldsymbol{\theta}_2$. In the period ambiguity case these models (as well as the parameter vectors) are functionally the same for both alternative models, the only difference is due to the different values of the frequency (which is embedded inside $\boldsymbol{\theta}_{1,2}$). Nonetheless we still use a bit more general notation than is necessary for our aliasing case. In general, $\boldsymbol{\theta}_1$ and $\boldsymbol{\theta}_2$ may be even unrelated to each other, having different dimensions. Given the timings t_i , measurements x_i , and expected (known) measurement uncertainties σ_i (for $i = 1, 2, \dots, N$), we may assume (just for some definiteness) that the probability density function of each measurement is Gaussian:

$$f_1(x_i|t_i, \sigma_i, \boldsymbol{\theta}_1) = \frac{1}{\sigma_i \sqrt{2\pi}} \exp \left[-\frac{1}{2} \left(\frac{x_i - \mu_1(t_i, \boldsymbol{\theta}_1)}{\sigma_i} \right)^2 \right], \quad (1)$$

with a similar definition f_2 for the second rival model, μ_2 . For further shortness, we define the pairs $z_i = \{t_i, \sigma_i\}$ and two vectors: \boldsymbol{x} containing all x_i and \boldsymbol{z} containing all z_i (that is, t_i and σ_i). These model probability density functions $f_{1,2}$ depend on the unknown vectors of parameters $\boldsymbol{\theta}_{1,2}$, which can be estimated from the data using the maximum-likelihood approach, which turns into the least-square one in the Gaussian case. Namely, the necessary estimations of $\boldsymbol{\theta}_{1,2}$ can be defined as

$$\hat{\boldsymbol{\theta}}_k = \arg \max_{\boldsymbol{\theta}_k \in \Theta_k} \mathcal{L}_k(\boldsymbol{x}|\boldsymbol{z}, \boldsymbol{\theta}_k) = \arg \min_{\boldsymbol{\theta}_k \in \Theta_k} \chi_k^2(\boldsymbol{x}|\boldsymbol{z}, \boldsymbol{\theta}_k), \quad (2)$$

where the functions

$$\begin{aligned} \mathcal{L}_k(\boldsymbol{x}|\boldsymbol{z}, \boldsymbol{\theta}_k) &= \prod_{i=1}^N f_k(x_i|z_i, \boldsymbol{\theta}_k), \\ \chi_k^2(\boldsymbol{x}|\boldsymbol{z}, \boldsymbol{\theta}_k) &= \sum_{i=1}^N \left(\frac{x_i - \mu_k(t_i, \boldsymbol{\theta}_k)}{\sigma_i} \right)^2 \end{aligned} \quad (3)$$

represent the appropriate likelihood functions and the chi-square functions, respectively. Note that the likelihood function also represents the joint probability density for the vector of the observables \boldsymbol{x} , given fixed timings, error uncertainties, and model parameters.

Let us now try to rigorously compare the two alternative models. Vuong (1989) suggests to use the Kullback-Leibler Information Criterion (KLIC) to compare the models in the sense of their separation from the truth:

$$\begin{aligned} \text{KLIC}_k(\boldsymbol{\theta}_k) &= \int \log \frac{h(x|z)}{f_k(x|z, \boldsymbol{\theta}_k)} h(x, z) dx dz = \\ &= \mathbb{E}_{\boldsymbol{x}, \boldsymbol{z}}^0 \log \frac{h(x|z)}{f_k(x|z, \boldsymbol{\theta}_k)}, \\ \text{KLIC}_{12}(\boldsymbol{\theta}_1, \boldsymbol{\theta}_2) &= \text{KLIC}_2(\boldsymbol{\theta}_2) - \text{KLIC}_1(\boldsymbol{\theta}_1) = \\ &= \int \log \frac{f_1(x|z, \boldsymbol{\theta}_1)}{f_2(x|z, \boldsymbol{\theta}_2)} h(x, z) dx dz \\ &= \mathbb{E}_{\boldsymbol{x}, \boldsymbol{z}}^0 \log \frac{f_1(x|z, \boldsymbol{\theta}_1)}{f_2(x|z, \boldsymbol{\theta}_2)}, \end{aligned} \quad (4)$$

where $h(x, z)$ represents the true (unknown) joint probability density of a single measurement x and of the associated quantities in z , and $h(x|z)$ is the respective conditional density of x given z . This true distribution h involves, the true signal shape and true error distribution shape, instead of the modelled ones. The quantities KLIC_1 and KLIC_2 assess the separation¹ between one of the two available statistical models of the data and the truth. The difference between these quantities, KLIC_{12} , measures the ability of the first model to reproduce the true distribution, relatively to the second one. The definitions in (4) do not yet involve anything from the actual observational data, they are defined regardless of what we observe. The symbol \mathbb{E}^0 denotes the mathematical expectation, taken for the true distribution h .

It is not required that the model error distribution shape set in the functions f_k should be close to h . In practice, we usually have no other option than to set f_k to the Gaussian functional shape (1). Then KLIC_{12} will measure the separation between μ_1 and μ_2 in the sense of their expected mean-square residuals. Such separation measure remains quite sensible and justified even when $h(x|z)$ is non-Gaussian. Moreover, even if we know definitely the non-Gaussian shape of h , we may want to compare the models in a homogeneous manner, still using the mean-square residual for this goal, i.e. assuming Gaussian f_k . We may want to avoid any binding to the true shape of h as much as possible, because it is often related only to instrumental properties rather than to physical objects that we observe.

In general, there is no “true” values of $\boldsymbol{\theta}_1$ and $\boldsymbol{\theta}_2$ that we could substitute in (4), since both rival models $f_{1,2}$ are

¹ We say “separation” instead of “distance”, since this divergence measure does not satisfy all necessary axioms of the distance, e.g. it is not symmetric and does not satisfy the triangle inequality.

wrong and the true distribution h is not parametrized at all. We should substitute the so-called “pseudo-true” values of θ_1 and θ_2 , which represent some theoretically most suitable values of these parameters. They are defined as the points where KLIC_1 or KLIC_2 reaches their maximums. Since the true density $h(x, z)$ is unknown, the pseudo-true values of $\theta_{1,2}$ are unknown too, but the estimations (2) can approximate them. Eventually, we want to test the null hypothesis $\text{KLIC}_{12} = 0$ (the two models are equally close to the truth) against the alternative $\text{KLIC}_{12} \neq 0$.

It is essential that in the definition (4) the timings and error uncertainties inside z_i are treated as random quantities too, so we can speak of the joint density $h(x, z)$. Such probabilistic interpretation of apparently non-random quantities is in fact quite natural, and we consider it as a strength of the approach. In practice, we often do not know the exact time of each observation in advance. This time depends on many things that are unrelated to the astronomical problem, like the observatory’s time allocation policy and current routine circumstances, the racing between different observing programmes, etc. This issue is also discussed in more details in Appendix A. It is important that we are not required to specify/estimate $h(x, z)$ explicitly, the test will deal with it automatically. Also, we do not make any restrictive assumptions about the distribution of the timings t_i : it is allowed to be highly non-uniform, e.g. gapped (as it usually occurs in astronomy).

Now, it is not difficult to realize that the following normalized log-likelihood ratio

$$L = \frac{1}{N} \log \frac{\mathcal{L}_1(\mathbf{x}|\mathbf{z}, \hat{\theta}_1)}{\mathcal{L}_2(\mathbf{x}|\mathbf{z}, \hat{\theta}_2)} = \frac{1}{N} \sum_{i=1}^N l_i, \quad l_i = \log \frac{f_1(x_i|z_i, \hat{\theta}_1)}{f_2(x_i|z_i, \hat{\theta}_2)} \quad (5)$$

represents an empirical estimation of the KLIC divergence measure (4), since the averaging over l_i approximates the mathematical expectation in (4). Note that the individual terms l_i are generated by the real data, so they are automatically averaged on the basis of the unknown true distribution h . This trick is rather reminiscent of the well-known jack-knife or bootstrap procedures, which also use the original sample to eliminate the necessity to specify the unknown error distribution.

Furthermore, we can find the empirical variance of l_i as

$$v^2 = \frac{1}{N} \sum_{i=1}^N l_i^2 - \frac{1}{N^2} \left(\sum_{i=1}^N l_i \right)^2. \quad (6)$$

The uncertainty of L is then equal to v/\sqrt{N} , and therefore the final Vuong statistic represents another re-normalised log-likelihood ratio

$$\mathcal{V} = \frac{L\sqrt{N}}{v} = \frac{\sum_{i=1}^N l_i}{\sqrt{\sum_{i=1}^N l_i^2 - \frac{1}{N} \left(\sum_{i=1}^N l_i \right)^2}}. \quad (7)$$

Under the null hypothesis, \mathcal{V} behaves asymptotically (for $N \rightarrow \infty$) as a standard normal variable (mean zero, variance unit). This result can be used to test the models equivalence. If $|\mathcal{V}|$ is too large then our null hypothesis $\text{KLIC}_{12} = 0$ is inconsistent with the data, so that the rival models are well-distinguishable and we can safely adopt the one which offers a better likelihood (i.e., the first one if $\mathcal{V} > 0$, or the second one otherwise). If \mathcal{V} is not large enough then we have to acknowledge that for now it is still too risky to choose between

the alternatives and it is better to seek for more data before drawing any definite conclusion. Given an observed value of \mathcal{V} , we can calculate the associated false alarm probability as $\text{FAP} = 2\Phi(|\mathcal{V}|)$, where $\Phi(x)$ is the standard Gaussian tail function (i.e., probability for a standard normal variable to exceed a given x). To reject the null hypothesis, we need to have this FAP below some small critical value FAP_* (typically, 1%, 5%, etc.).

The formula (7) actually refers to the case when both models have the same number of free parameters (degrees of freedom). If it is not the case, we need to add a minor bias correction, because models with larger number of parameters always produce systematically better fits than models with smaller number of parameters. Vuong (1989) suggests to add a Bayesian-style correction as

$$\mathcal{V} = \frac{\sum_{i=1}^N l_i - \frac{d_1 - d_2}{2} \ln N}{\sqrt{\sum_{i=1}^N l_i^2 - \frac{1}{N} \left(\sum_{i=1}^N l_i \right)^2}}, \quad (8)$$

with d_1 and d_2 being the numbers of free parameters in the models. This correction tends to zero when $N \rightarrow \infty$, although may remain relatively important in practice, especially when $d_1 - d_2$ is large.² In this paper we only deal with models having the same number of parameters, so we will use only the uncorrected formula (7).

Since the Vuong test is based on the usual likelihood ratio statistic, it is interesting to compare it with the traditional methods for testing nested hypotheses, when the first model represents a parametric subspace of the second one. This traditional problem basically represents a degenerate case in the conditions of the non-nested hypotheses testing, and the distribution of \mathcal{V} is then not asymptotically normal. It is well-known that in that case the quantity LN follows a chi-square distribution (if the first model is correct). As it is discussed in the previous paragraphs, in the non-nested case the quantity $L\sqrt{N}$ is asymptotically normal. Therefore, the main difference between the nested and non-nested situations is in the magnitude of the random scatter in L , about $\sim 1/N$ or about $\sim 1/\sqrt{N}$.

We need to emphasize that the Vuong statistic is not equivalent to the textbook likelihood ratio in (5). The only common thing between L and \mathcal{V} is their sign. This means that the Vuong test uses in fact the likelihood function to identify which of the models is more likely. However, as we explained in Sect. 2, our main goal was to find out whether the alternatives are distinguishable or they are not. The likelihood ratio method is not usable for this, because its distribution in this situation is not known in general. It is only known that the distribution of L is asymptotically normal, but its variance is severely dependent on the particular data/error model in f , and should be evaluated on the task-by-task basis (Cox 1962). The Vuong test involves a normalization that makes the distribution of \mathcal{V} asymptotically invariable with respect to the model f .

² When passing to the limit $N \rightarrow \infty$, the values of L in (5) and v in (6) tend to certain constant finite values. Namely, L tends to the KLIC defined in (4), and v tends to a similar expression with mathematical expectation replaced by the variance operator. Bearing this in mind, we easily find that the difference between (7) and (8) decreases as $\ln N/\sqrt{N}$.

Another very important consequence is that the Vuong test is asymptotically insensitive to possible model faults, in the sense that \mathcal{V} preserves its standard normal distribution even if the true signal and error behaviour does not really match the model f . Such possible shortcomings of f may have two distinct reasons: (i) wrong assumptions about the signal shape and (ii) wrong assumptions about the measurement error distribution.

In the first case, we try to fit the observed signal using inadequate models. In this case our test cannot suggest any third (correct) model, this task still lies on the researcher's shoulders. However, it can advice us whether the models at disposal are distinguishable or equivalent. The answer to this question is often important even for inaccurate models, because if these simpler models are indistinguishable then there is a little chance that some other more complicated model may appear more suitable (and at least observationally distinguishable from the original models). In this case, it is important that both Vuong test does not assume that any of the available alternatives is true (while, e.g., in the classic base/alternative hypothesis testing it is always assumed that either first or at least the second model is functionally correct).

In the second case, we may assume inadequate model for the error distribution. This is not an obstacle for our test at all: the asymptotic distribution of the statistic \mathcal{V} remains the same for the most well-behaving distributions of the measurement errors (possibly except for some too heavy-tailed ones that always constitute a trouble, see all rigorous formulation in Vuong 1989). As we noted above, in practice it is even desirable not to bind our ordering criterion (KLIC) to the shape of the error distribution, since this shape is usually related to the instrumental characteristics rather than to the physical phenomenon under study. For example, setting f to a Gaussian bell shape (1) we always order our signal models in the sense of the mean-square deviation. When f does not match the true shape of the error distribution, the quantity in Eq. (5) and, consequently, \mathcal{V} are related to the so-called pseudo maximum-likelihood tests that possess many practically useful properties of the classic likelihood ones (Gourieroux et al. 1984; Baluev 2009).

Nonetheless, the Vuong (1989) paper contains a possibly essential requirement of the statistical independence of the pairs (z_i, x_i) for different i . Therefore, both the Vuong test may yield unreliable results, if the measurement noise is correlated (not white).

4 PRACTICAL FORMULAE

For the Gaussian distribution (1), the Vuong statistic can be derived from (7), substituting

$$l_i = \frac{(\hat{\mu}_1(t_i) - \hat{\mu}_2(t_i))}{\sigma_i^2} \cdot \left[x_i - \frac{\hat{\mu}_1(t_i) + \hat{\mu}_2(t_i)}{2} \right],$$

$$\hat{\mu}_1(t) = \mu_1(t, \hat{\theta}_1), \quad \hat{\mu}_2(t) = \mu_2(t, \hat{\theta}_2). \quad (9)$$

These formulae can be used after substitution of the best fitting alternative models $\hat{\mu}_1$ and $\hat{\mu}_2$ that we wish to compare (these models are task-specific).

In the simplified aliasing case, we have formally the same model for the both alternatives, which represents a sinusoidal oscillation:

$$\mu(t, \theta) = a \cos(\omega t) + b \sin(\omega t), \quad \theta = \{a, b, \omega\}. \quad (10)$$

The two alternatives are different only due to the different admissible ranges for the frequency: for the first model, μ_1 , the (circular) frequency ω should be located around the first rival frequency, $\hat{\omega}_1$, and for the model μ_2 it should be around $\hat{\omega}_2$. In practice, it is more convenient to treat μ_1 and μ_2 as different models, rather than two variants of the model (10), because of the strong non-linearity of the frequency parameter. The test that we have described has asymptotic nature (for $N \rightarrow \infty$), consequently it implicitly utilise some hidden linearisation of the models in the vicinity of the best fitting estimations. Although the coefficients a and b are fully linear for all values of ω , the frequency ω itself is not globally linear and is not linearisable in the global sense, although it is still linearisable in the local sense. Therefore, we should treat the basic model μ in the vicinities $\omega \simeq \hat{\omega}_1$ and $\omega \simeq \hat{\omega}_2$ as two separate models.

Let us write down the classical expression for the Lomb-Scargle periodogram:

$$z(\omega) = \frac{1}{2} \left[\frac{\left(\sum \frac{x_i}{\sigma_i^2} \cos \omega(t_i - \tau) \right)^2}{\sum \frac{1}{\sigma_i^2} \cos^2 \omega(t_i - \tau)} + \frac{\left(\sum \frac{x_i}{\sigma_i^2} \sin \omega(t_i - \tau) \right)^2}{\sum \frac{1}{\sigma_i^2} \sin^2 \omega(t_i - \tau)} \right],$$

$$\tan 2\omega\tau = \frac{\sum \frac{1}{\sigma_i^2} \sin 2\omega t_i}{\sum \frac{1}{\sigma_i^2} \cos 2\omega t_i}. \quad (11)$$

Note that τ is also a function of ω . As it is already well-known, the Lomb-Scargle periodogram is directly related to the likelihood ratio statistic, or, in the Gaussian case, to the chi-square statistic (Zechmeister & Kürster 2009; Baluev 2008). In addition to the periodogram itself, we will need the expressions for the associated best fitting coefficients a and b of the original model (10). They are given by

$$\hat{a}(\omega) = \frac{\sum \frac{x_i}{\sigma_i^2} \cos \omega(t_i - \tau)}{\sum \frac{1}{\sigma_i^2} \cos^2 \omega(t_i - \tau)},$$

$$\hat{b}(\omega) = \frac{\sum \frac{x_i}{\sigma_i^2} \sin \omega(t_i - \tau)}{\sum \frac{1}{\sigma_i^2} \sin^2 \omega(t_i - \tau)}, \quad (12)$$

and the final best fitting sinusoidal model evaluates to

$$\hat{\mu}(t, \omega) = \hat{a}(\omega) \cos \omega(t - \tau) + \hat{b}(\omega) \sin \omega(t - \tau). \quad (13)$$

From a preceding period analysis we should have already estimated the possible rival frequencies $\hat{\omega}_1$ and $\hat{\omega}_2$, which correspond to the two largest peaks of the periodogram. Substituting these frequencies in (13), we obtain the two best fitting models $\hat{\mu}_1(t)$ and $\hat{\mu}_2(t)$, which allow to evaluate all quantities l_i using (9), and then the Vuong statistic (7). In particular, it can be readily shown that

$$NL = \sum_{i=1}^N l_i = z(\hat{\omega}_1) - z(\hat{\omega}_2), \quad (14)$$

which is not surprising, since the sum of l_i represents the pure log-likelihood ratio statistic, and the Lomb-Scargle periodogram is tied to the log-likelihood function.

This is not yet the full story. In practice, the quantities

σ_i usually are not known with good precision, and we need to model them too. For instance, the multiplicative model $\sigma_i^2 = \kappa/w_i$ is widely used, where the factor κ is an extra unknown parameter, and w_i are the known statistical weights. In that case, the quantities l_i are more complicated, relatively to (9):

$$l_i = \frac{N}{2} \left(\frac{\widehat{\nu}_2(t_i)}{\widehat{\chi}_2^2} - \frac{\widehat{\nu}_1(t_i)}{\widehat{\chi}_1^2} \right) + \frac{1}{2} \log \frac{\widehat{\chi}_2^2}{\widehat{\chi}_1^2},$$

$$\widehat{\nu}_k(t) = w(t)(x(t) - \widehat{\mu}_k(t))^2, \quad \widehat{\chi}_k^2 = \sum_{i=1}^N \widehat{\nu}_k(t_i) \quad (15)$$

In the case of the sine curve (10) we obtain

$$NL = \sum_{i=1}^N l_i = \frac{N}{2} \log \frac{\widehat{\chi}_2^2}{\widehat{\chi}_1^2} = \frac{N}{N_{\mathcal{K}}} (z_3(\widehat{\omega}_1) - z_3(\widehat{\omega}_2)), \quad (16)$$

where the periodogram z_3 is defined in (Baluev 2008). The number $N_{\mathcal{K}}$ is equal to $N - d_{\mathcal{K}}$, where $d_{\mathcal{K}}$ is the number of free parameters in the full model with the probe sinusoid (10), excluding the frequency parameter. For the cases that we consider here we always have $d_{\mathcal{K}} = 2$ (two parameters a and b), but for more general cases, which involve an underlying variation in addition to the periodic signal (see Baluev 2008), the number $d_{\mathcal{K}}$ may be larger.

Finally, we may use another parametrization of the measurement uncertainties, like e.g. the so-called additive model $\sigma_i^2(p) = p + \sigma_{\text{meas},i}^2$ with a free parameter p , as considered in (Baluev 2009). In this case the formula for the quantities l_i will look like:

$$l_i = \frac{1}{2} \left[\left(\frac{x_i - \widehat{\mu}_2(t_i)}{\sigma_i(\widehat{p}_2)} \right)^2 - \left(\frac{x_i - \widehat{\mu}_1(t_i)}{\sigma_i(\widehat{p}_1)} \right)^2 \right] + \log \frac{\sigma_i(\widehat{p}_2)}{\sigma_i(\widehat{p}_1)}. \quad (17)$$

In this expression, $\widehat{p}_{1,2}$ represent the estimations of the parameter p associated to one of the models.

In practice, we will probably use more complicated signal models than a sinusoidal one, of course. Just for example, we might want to add to our sinusoidal model some underlying variation, e.g. a simple constant term or a linear or quadratic trend, as it is done in the generalized least-square periodogram described in (Baluev 2008; Zechmeister & Kürster 2009). We omit the detailed formulae for these cases, since they would be relatively bulky for a presentation here, and the reader can now easily derive them himself.

5 PRACTICAL APPLICABILITY OF THE METHOD

Considering a statistical test from the view point of its practical applicability, we usually ask two main questions,

(i) *Concerning the behaviour of the test under the null hypothesis:* How precisely we can estimate the false alarm probability, associated with an observed value of the test statistic?

(ii) *Concerning the behaviour of the test under the alternative:* Given an accurate FAP estimation, how sensitive is our test to practically expected deviations from the null hypothesis?

Both issues can be addressed by means of numerical simulations, which is the goal of this section.

5.1 Test reliability

For the first issue, we need to specify some model condition satisfying the null hypothesis, then run a Monte Carlo simulation procedure (generating artificial random measurement errors), counting how frequently we meet the false alarms (the events when our test wrongly rejects the null hypothesis), and then to compare the simulated significance value with the expected one. In our case, we need first to construct some test signal that produces two alternative observed periods, for which $\text{KLIC}_{12} = 0$. It is not so easy as it may seem, because simultaneously the rival periods should not be indistinguishable in principle. For example, for strictly evenly spaced observations, $t_i = i\Delta t$, each periodicity can be equally treated as having the original frequency ω or any alias frequency $\omega + 2\pi k/\Delta t$ for any integer k . All these alternative interpretations are fully equivalent and observationally indistinguishable under any circumstances, since they generate exactly the same sequence of values at t_i . The Vuong statistic is not defined for this case at all, because all l_i in (9) are identically zero. This is not the situation that we want to test, since in practice we need to compare only potentially distinguishable alternatives. As a more realistic test model, we can consider a non-degenerate aliasing (the data are gapped in time rather than strictly evenly spaced), an ω_0 -periodic signal, and its two primary aliases $\omega_{1,2} = \omega_0 \pm \omega_g$ (with ω_g being the data gapping frequency). If we neglect the main frequency ω , these peer aliases provide practically equal interpretation of the observations.³

Given this test model, we can generate a Monte Carlo sequence of mock time series by adding simulated random errors to the probe sinusoid and generating random timings according to the specified gapping pattern. In our case, N timings t_i were distributed uniformly within $n = 10$ periodically gapped intervals $[kP_g, (k+f)P_g]$, with $f \in [0, 1]$ being a filling parameter (fixed during each simulation series). For each such simulated data set, we evaluate the Vuong statistic \mathcal{V} comparing the two primary aliases near $\omega_0 \pm \omega_g$. After that, we compare the resulting simulated distribution of \mathcal{V} with the expected standard normal distribution.

The results of the simulations are shown in Fig. 1. In these diagrams, the axes show expected and simulated significance levels in the so-called n - σ notation, which is convenient when dealing with normal or almost normal probabilities. For the expected significance (in the abscissas) this is just equal to an observed value of $|\mathcal{V}|$. Each value in the ordinates, S , represents such critical value for a hypothetical standard normal variable x that the probability for $|x|$ to exceed S is equal to the actual simulated probability for $|\mathcal{V}|$ to exceed the value in the abscissa. Larger S implies higher significance level and smaller FAP.⁴ If \mathcal{V} indeed follows the

³ The cases when the true signal period is never taken into account are not really artificial. For example, the true orbital period of 0.7 days for the extrasolar planet 55 Cnc e was hidden for a very long time behind an alias of 2.8 days (Dawson & Fabrycky 2010). This happened only because the researchers did not plot the periodograms beyond the 1 day period bound, until recent time.

⁴ We remind that the frequently used one-, two-, and three-sigma levels correspond to $\text{FAP} = 31.7\%$, 4.6% , and 0.27% , and in general $\text{FAP} = 2\Phi(S)$.

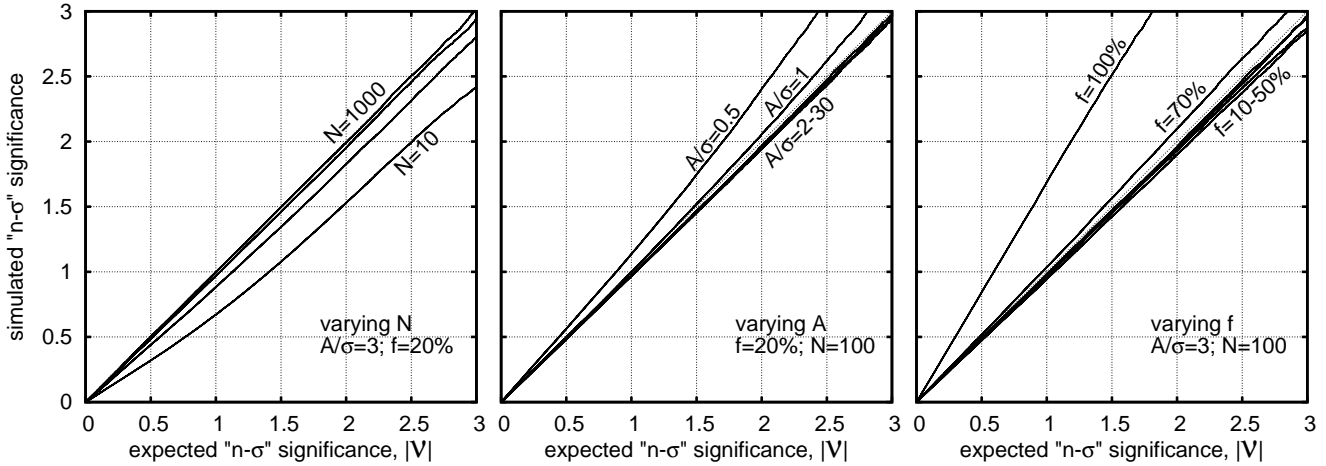


Figure 1. Predicted vs. simulated significance levels for the Vuong test, depending on various parameters. Abscissas show the absolute value of the Vuong statistic, while the ordinates show the actual (simulated) significance level in the “ n - σ ” notation. If the Vuong statistic was perfectly normal then the simulated significance level would be $S(|\mathcal{V}|) = |\mathcal{V}|$, and the corresponding graph would strictly follow the diagonal line. See text for further details.

expected standard normal distribution then $S(|\mathcal{V}|) = |\mathcal{V}|$, and its graph should strictly follow the main diagonal. If, for instance, \mathcal{V} has some non-unit variance $\sigma_{\mathcal{V}}^2$ and still normal then $S(|\mathcal{V}|) = |\mathcal{V}|/\sigma_{\mathcal{V}}$.

In Fig. 1 we show the graphs of $S(|\mathcal{V}|)$ varying different parameters of the test model. Overall, the agreement between simulated and expected significances is good, except for certain rather boundary cases. The bad cases include: small number of the observations $N \lesssim 30$, very small signal amplitude $A \lesssim \sigma$, or too weak aliasing $f \gtrsim 70\%$. The two latter bad cases correspond to a small signal/noise ratio of the aliases involved, so that we even cannot be sure that at least one of them is actually significant. For example, $f = 100\%$ corresponds to no aliasing at all, when the two rival aliases in our test model are destroyed. Then the test attempts to compare noisy peaks which appeared in these positions occasionally. Such cases are not practical, since in practice the significance of at least one of the alternatives is already established before we ask which one is true.

Summarizing these results, we can derive the following empiric condition of the Vuong test applicability:

$$A'/\sigma \gtrsim \sqrt{N_0/N}, \quad (18)$$

where A' is the best fitting amplitude of the rival periodicities, and N_0 is a constant. The amplitude A' is smaller than the amplitude A of the original generating signal, since A' refers to the alias periodicities, while the main period is neglected. For our gapped time series we can readily obtain an analytic approximation for A' using the classical period analysis formulae (e.g. Vityazev 2001):

$$A' \simeq A \frac{\sin \pi f}{\pi f}. \quad (19)$$

In practice, it is more convenient to deal with the corresponding periodogram peak value rather than with the best fitting signal amplitude. We can rewrite (18) in a very simple form

$$z' \simeq \frac{A'^2 N}{4\sigma^2} \gtrsim z_0 = \frac{N_0}{4}. \quad (20)$$

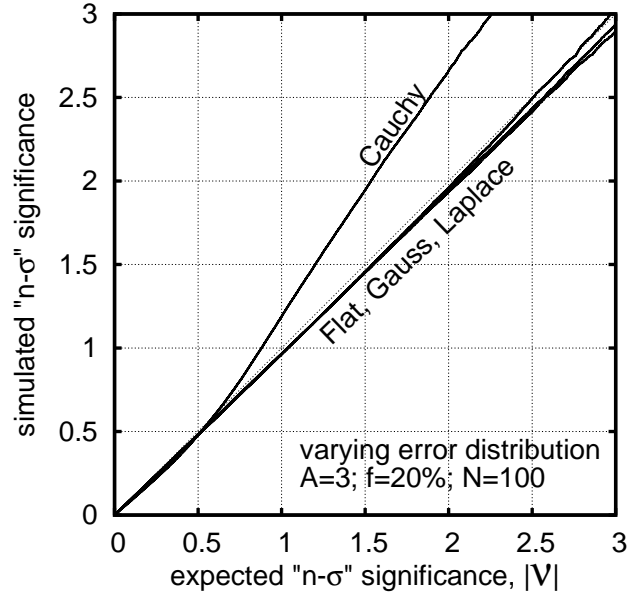


Figure 2. Predicted vs. simulated significance levels for the Vuong test, depending on the true error distribution. The notes from Fig. 1 apply here. Always assuming the Gaussian model (1) in the Vuong test, we perform simulations using several non-Gaussian error models: flat p.d.f. in the range $[-1, 1]$, Laplace p.d.f. $\propto e^{-|x|}$, and Cauchy p.d.f. $\propto 1/(1+x^2)$. Only the Cauchy distribution causes significant effect on the statistic \mathcal{V} .

When applying (20) in practice, we should simply check whether the rival periodogram peaks that we want to compare are both above the z_0 level. For our test problem, we find $N_0 \simeq 50$ and $z_0 \simeq 10$, although we must note that these thresholds may increase when e.g. we compare highly non-linear models.

So far we assumed that the measurement errors distribution is always Gaussian. What if in true this distribution is

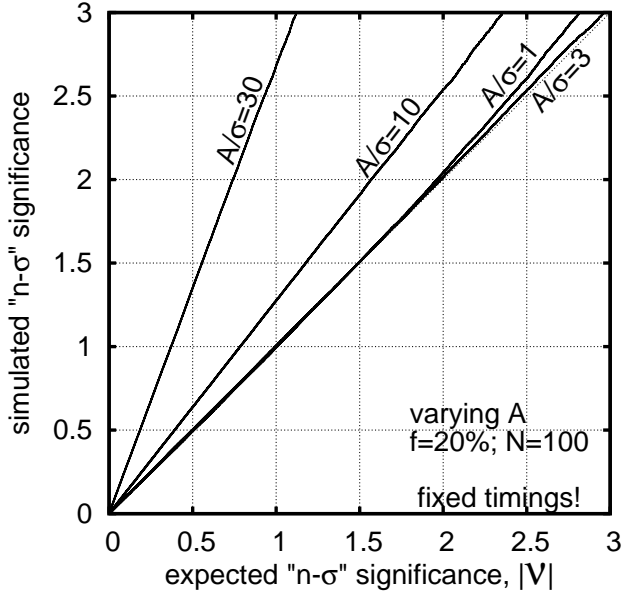


Figure 3. Predicted vs. simulated significance levels for the Vuong test, assuming fixed timings t_i . The notes from Fig. 1 apply here. Here we vary only the signal amplitude.

different from the one used in the Vuong test? Theoretically, the behaviour of the Vuong test should remain basically the same (in the most cases). This is verified by the simulations presented in Fig. 2. We can see that most error distribution that we tried out did not introduce any significant changes indeed. Only the Cauchy distribution produced some large systematic effect. This is not very surprising, because various peculiarities of the asymptotic behaviour are typical for the Cauchy distribution, due to its heavy tails.

It is also interesting to investigate the case of fixed t_i (Fig. 3). In this case, the distribution of the Vuong statistic may become significantly more concentrated, in comparison with the random t_i case. We find that the main critical parameter in this case is the signal amplitude. For small A , the distribution of the Vuong statistic does not depend much on whether we assume fixed or random timings. For large A , the scatter of the Vuong statistic shrinks, and the simulated significance level for the fixed t_i becomes larger than for the random t_i . This probably occurs because large amplitude scales up the sensitivity of l_i in (9) to the small fluctuations in t_i . It is practically important that the standard normal distribution still allows us to assess a *lower* bound on the significance of $|\mathcal{V}|$. This means that the number of false alarms still remains limited according to our request, although it may appear smaller. In addition, the cases of large amplitude are not very important, since in practice a period ambiguity is rare when the signal is so strong. We would like to emphasize that in practice the timings t_i indeed usually have random nature that should not be neglected.

5.2 Test efficiency

Now let us consider the second main issue – the sensitivity of the Vuong statistic to the cases when one rival model is indeed better than the another one. In this case, we may

consider the same sinusoidal test signal and simply compare the main period with one of the aliases, e.g. the primary one having frequency $\omega_0 + \omega_g$. The average value of \mathcal{V} should be now biased to positive values, since the first (correct) model should look systematically more likely. For each simulation trial, we may have three types of outcomes: a success ($|\mathcal{V}|$ exceeds some positive critical value \mathcal{V}_* and \mathcal{V} is positive too), a failure ($|\mathcal{V}| > \mathcal{V}_*$ but $\mathcal{V} < 0$), and a neutral (inconclusive) outcome ($|\mathcal{V}| < \mathcal{V}_*$). We denote the respective probabilities as P_s , P_f , and P_i . All of them are functions of the critical level \mathcal{V}_* , which can be tied to the rejection significance level $S(\mathcal{V}_*) \approx \mathcal{V}_*$ or to the corresponding false alarm probability. Speaking in terms of Section 2, the quantities P_f , P_i , and FAP represent the probabilities to make the first, second, or third kind mistake. In addition, we can now define a few other indicators of the test performance: the failures/successes probabilities ratio, FS, the failures/inconclusives ratio, FI, and the successes/inconclusives ratio, SI. Obviously,

$$\begin{aligned} 1/P_s &= 1 + \text{FS} + \text{SI}, \\ 1/P_f &= 1/\text{FS} + 1/\text{FI} + 1, \\ 1/P_i &= 1 + 1/\text{SI} + \text{FI}, \\ \text{FI} &= \text{FS}/\text{SI}. \end{aligned} \quad (21)$$

Only two variables involved in these equalities can be treated as independent. We choose to use FS and SI as these basic characteristics. These two quantities characterise, how frequent are mistakes of the first and second kind, in comparison with successful classifications (given fixed probability of the third kind mistakes, FAP). The quantity FS can be also interpreted as a measure of how much our test exceeds a simple drop of a coin (which has FS = 1). The quantity SI measures the test conservativeness. A perfect test should possess small values of FS and SI.

Together with the requested significance level, we now have three independent characteristics FS, SI, and S , which are all functions of a single control parameter – the critical value \mathcal{V}_* . Therefore, to fully characterise the test performance, we should investigate the corresponding parametric curve in the three-dimensional space (FS, SI, S). This is a bit more complicated than, for example, in the usual signal detection task, when we have only two independent variables — the false alarm probability and the probability of wrong non-detection. We therefore have no other option than to deal with some two-dimensional projections. Since the behaviour of $S(\mathcal{V}_*) \approx \mathcal{V}_*$ has been already investigated in details, we now look at the pair (FS, SI).

In the Fig. 4 we plot several graphs of $(\text{SI}(\mathcal{V}_*), \text{FS}(\mathcal{V}_*))$ as parametric curves, setting different values for the signal and time series parameters. On each curve we also mark a few points corresponding to the values of \mathcal{V}_* from 1 to 3. As we could expect, increasing the signal amplitude A , or the number of observations N , or the time series filling factor f decreases both the probability of a misclassification and of an inconclusive result. We may note that when varying different control parameters we usually obtain very similar curves. This indicates that there should be a single quantity (a combination of N , A , and f) that defines the test performance for our task. On the basis of the presented simulations, we can empirically construct this critical quantity as

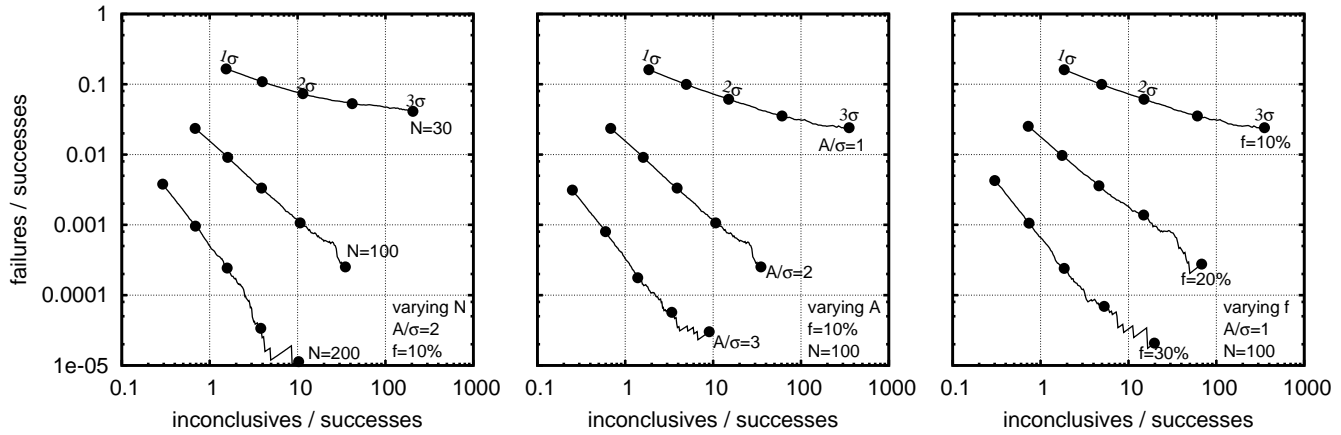


Figure 4. Simulated performance of the Vuong test, depending on various parameters. Here we inspect the behaviour of the Vuong statistic comparing the primary (“true”) peak near the main frequency ω_0 and its alias near $\omega_0 + \omega_g$ (the exact values were adjusted to achieve a local maximum of the periodogram). In each curve we also put five points marking the positions of $\mathcal{V}_* = 1, 1.5, 2, 2.5, 3$, which approximately correspond to the same significance levels (S), i.e. from one-sigma to three-sigma. The “failures” refer to the cases when the Vuong test suggested to select the alias peak. The number of Monte Carlo simulations was 10^6 . See text for further details.

$$G \simeq \frac{A}{\sigma} f \sqrt{N}. \quad (22)$$

Three curves in each panel of the Fig. 4 correspond to $G \approx 1$, $G \approx 2$, and $G \approx 3$. The formula (22) can be also justified theoretically. Indeed, since the Vuong statistic is based on the quantity L , which is expressible as the difference (14) between two rival periodogram values, the latter difference should represent a critical parameter characterising the test performance. For the primary peak and its alias, this difference looks like

$$\begin{aligned} z_1 - z_2 &\simeq N \frac{A^2 - A'^2}{4\sigma^2} \simeq \frac{A^2 N}{4\sigma^2} \left[1 - \left(\frac{\sin \pi f}{\pi f} \right)^2 \right] \simeq \\ &\simeq \frac{A^2 \pi^2 f^2 N}{12\sigma^2} = \frac{\pi^2}{12} G^2. \end{aligned} \quad (23)$$

This is not a rigorous proof of (22), however.

We can see that the Vuong test can manage the misclassification errors very well, but it favours a relatively large number of inconclusive results. This is not very surprising, since this test is originally designed to be conservative in drawing definite conclusions. This is the main reason why it suppresses the misclassifications so efficiently. From the presented simulation results, we may also note that in practice it does not make much sense to request very high significance level from the Vuong test. Requesting large value of $S(\mathcal{V}_*)$ can further suppress the third-type mistakes, but by the cost of a dramatic increase in the fraction of inconclusive results, which can even become dominating. Simultaneously, the relative fraction of the first-type mistakes (misclassifications) either is not decreased very much or is already sufficiently small for moderate S . Therefore, we believe that in practice it is enough to set the required significance level about 1.5 – 2 sigma.

In practice we often deal with more complicated situations, however. In addition to the true period, we may have also *multiple* aliases, and there is no guarantee that the true period is indeed associated to one of the two largest pe-

riodogram peaks. Both selected highest peaks may occur aliases. In that case, we need to answer a principal question: what event we should treat as a failure of the test? Apparently, a failure should occur each time when the test suggests to choose an alias period. However, testing for multiple alternatives is not the responsibility of the Vuong test. The only thing that we required from this test, by its design, is to choose a *better* solution among the *two* ones provided on input. From this view point, the failures only occur when the test suggests to choose the peak which is more distant from the true period than the alternative candidate. The cases when the test selects an alias peak, while the second candidate is a larger-order alias, should be treated as successes (even if the selected peak is an alias too).

We performed simulations for both interpretations. To increase the contrast, we also added some penalty in the first interpretation, counting each selected k -order alias near $\omega = \omega_0 \pm k\omega_g$ as k failures at once. The results appeared apparently the same, however. This indicates that the cases, when both the largest periodogram peaks are only aliases, are rare and usually trigger an inconclusive decision of the Vuong test. The results of the simulations are shown in Fig. 5. In fact, this figure differs from Fig. 4 mainly because it is now allowed to choose any of the two first-order aliases near $\omega_0 \pm \omega_g$, instead a single alias alternative $\omega_0 + \omega_g$. A high-order alias may be selected too, but, as we have just discussed, the probability of such an event appears negligibly small. Comparing Fig. 5 with Fig. 4, we note two main differences. First, the fraction of inconclusive results is increased, as well as its sensitivity of the requested value of \mathcal{V}_* . Second, the threshold value of G , necessary to suppress these inconclusive decisions, grew roughly by half, and the sensitivity of the simulated curves to the value of G is also increased. To have, say, only half of inconclusive decisions, given 1.5-sigma or 2-sigma confidence level (S), the value of G should be about 4.5 or 3.5.

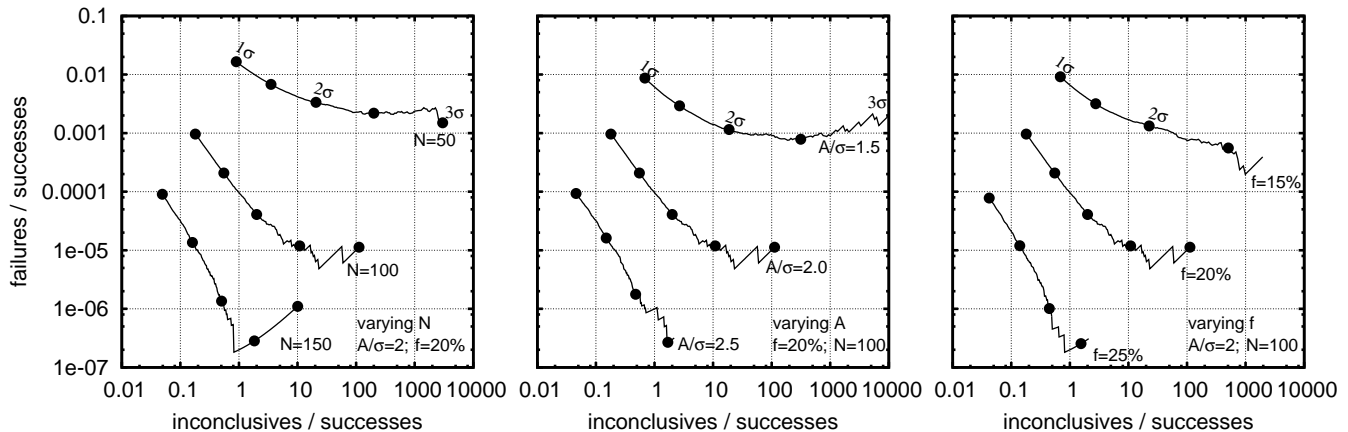


Figure 5. Simulated performance of the Vuong test, depending on various parameters. Similar to Fig. 4, but instead of picking two given periodogram peaks (the main one and a given alias) we now inspect two *largest* peaks among *many* period candidates near $\omega_0 + k\omega_g$. The parts of the curves corresponding to \mathcal{V}_* values between 2.5 and 3 are very unreliable here, regardless a larger number of Monte Carlo simulations (10^7). These curves appeared apparently the same for two different definitions of a “failure”: (i) the cases when the Vuong test recommends to select a peak, while the second candidate is actually better, and (ii) the cases when the Vuong test recommends to select any alias peak (not the true one). In the second interpretation, selecting a k^{th} -order alias was counted as k failures at once. The plotted curves are for the first interpretation. See text for further details.

6 APPLICATIONS

6.1 Exoplanetary system orbiting 55 Cnc

For many years it was believed that the planet 55 Cnc *e*, the innermost planet in the 55 Cnc system, possesses an orbital period of $P_e \approx 2.8$ day, until Dawson & Fabrycky (2010) showed that this apparent periodicity is actually a diurnal alias of the true one with $P_e \approx 0.7$ day. This new period value allows for a significantly better fit of the available data. This true period value could hide for so long time only because the researchers did not consider any potential periods smaller than 1 day. Here we would like to rigorously compare these alternative period values utilising our new method. We use Lick and Keck radial velocity data from (Fischer et al. 2008) to obtain two alternative five-planet fits with $P_e \approx 0.7$ day or $P_e \approx 2.8$ day. With the use of multi-Keplerian (unperturbed) model of the radial velocity we obtain $\mathcal{V} \approx 5.6$ for these alternatives. Using N -body Newtonian radial velocity model, as described in (Baluev 2011), we have $\mathcal{V} \approx 5.5$ (assuming the system is seen edge-on). No doubts, the period of 0.7 day is indeed the correct one.

We may also carry out another, somewhat unusual, model comparison. Estimated planetary orbital parameters and masses, as well as the fit quality, are a bit different for Keplerian and Newtonian models of radial velocity. So we might ask: are these differences statistically significant? In other words, can we say that mutual planetary perturbations are already detected in the RV data? To answer this question, we just need to find two orbital fits, one using Keplerian and another using Newtonian model, and then to calculate the Vuong statistic for these models. We obtain \mathcal{V} of only 0.2. Allowing for the common orbital inclination to the sky plane to float during the fitting, we get $\mathcal{V} \approx 0.4$ (with the best fitting inclination of 16°). So small values of \mathcal{V} say that possible gravitational perturbations in this system are not yet detectable from RV curve. Therefore, any attempt

to constrain orbital inclinations in this system from the RV data (on the basis of potential interplanetary perturbations) would be probably meaningless, possibly except for putting some very mild and thus not too much useful limits.

6.2 Exoplanetary system orbiting HD75898

This star was observed by the Keck team (Robinson et al. 2007), who reported the discovery of a Jovian-mass planet having orbital period of about 400 days. The relevant periodogram shows actually two comparable peaks at the periods of 400 days and 200 days (see Fig. 6). Let us try to verify the results by Dawson & Fabrycky (2010), who investigated this aliasing ambiguity more carefully and confirms that the 200-day period should be rejected indeed. We basically agree: $\mathcal{V} \approx 3.5$ in this case, so we can safely choose the period of 400 days, since the difference between the models has very high significance of more than 3σ .

6.3 Exoplanetary system orbiting GJ876

The planetary system orbiting GJ876 is currently believed to host four planets (Rivera et al. 2010). The detailed analysis of all up-to-date radial velocity data for this system, including recent HARPS (Correia et al. 2010) and Keck (Rivera et al. 2010) data, is given in (Baluev 2011), along with the full orbital configuration details. Here we would like to consider two ambiguities associated to this planetary system.

The first issue is related to the orbital period of the innermost planet GJ876 *d*. Since the very discovery of this planet it was noted (Vogt et al. 2005) that (presumably) the primary period value $P_d \approx 1.938$ day is accompanied by a diurnal alias of $P_d \approx 2.055$ day. The analysis done by Dawson & Fabrycky (2010) supports this classification, as well as our calculations, which yield $\mathcal{V} \approx 2.0$ for this alias

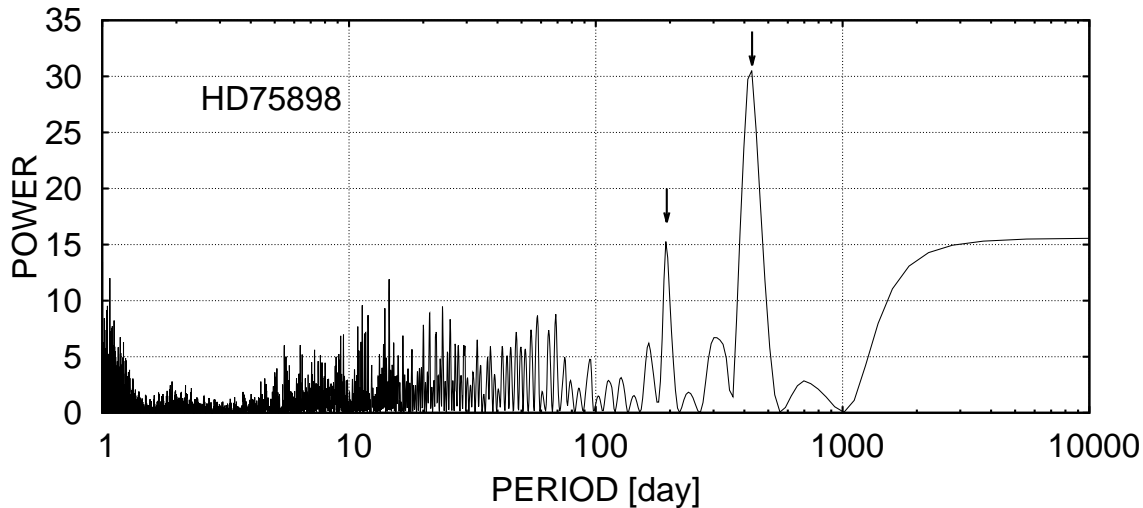


Figure 6. Periodogram of HD156668 radial velocity data, showing two high peaks at the period values of 400 days and 200 days. The Vuong test suggests that these peaks are distinguishable at 3.5σ level, thus we may definitely accept the peak at 400 days as the correct solution for the planet *b*. Here we perfectly agree with Dawson & Fabrycky (2010).

ambiguity. Therefore, here we are able to rigorously confirm that these periods indeed are well-distinguishable and the correct period is 1.938 day.

The second issue that we would like to highlight concerns the determinability of the planet GJ876 *e* eccentricity, e_e . It is noted in (Baluev 2011) that this eccentricity, although is bounded by ~ 0.2 from the upper side, looks still ill-determined below this limit. In particular, we have two comparable local minima of the likelihood function: the first one at $e_e \approx 0$ and another at $e_e \approx 0.15$ (with the corresponding pericenter argument $\omega_e \sim 45^\circ$). Therefore, this ambiguity looks like a good task suitable for the statistical methods proposed in the present paper. We find that the Vuong test agrees that these two orbital solutions are observationally indistinguishable: \mathcal{V} varies within the range of $0.5 - 1$, depending on some minor model details. This result allows us to confirm more rigorously the conclusion that e_e is indeed ill-determined.

As it is shown in (Baluev 2011), both HARPS and Keck data for GJ876 contain significant autocorrelated component (red noise). We must acknowledge that this red noise could make the Vuong test not very reliable, because such measurements are not uncorrelated. Nevertheless, in practice taking this red noise into account usually *increases* various statistical uncertainties, so apparently distinguishable models could appear actually equivalent, but hardly vice versa.

We do not believe, however, that this red noise could affect our previous disambiguation of the planet *d* period. The two alternatives for this period reside very close to each other, while the effect of the correlated noise is spread over the whole frequency spectrum. It could distort the balance between some distant periodogram peaks, but not between these ones.

6.4 Exoplanetary system orbiting GJ3634

According to Bonfils et al. (2011), this star is orbited by a super-Earth planet each 2.6 day. As the discoverers note, in

Table 1. Comparing three alias alternatives for GJ3634 *b*: values of \mathcal{V} obtained for various alias pairs

Alias	1.60 d	2.67 d
2.65 d	1.8	2.4
1.60 d	—	0.8

addition to the periodic signature of this planet, the radial velocity data also contain a parabolic long-term drift. The periodogram of the RV data with this trend removed (that is, included in the base model) is shown in Fig. 7. This periodogram shows two apparent peaks, with the peak at approximately 2.6 days being actually double, consisting of a close pair at the periods of 2.65 day (height 32) and 2.67 day (height 18). The discovery team does mention the period of 1.6 day, but they just retract it as an alias without any rigorous justification. They also do not mention that the peak at 2.6 day is double. The results of our analysis are given in Table 1, where each cell contains a numerical value of \mathcal{V} , comparing the aliases marked in the left column and in the top line. We can see that the peak at 2.67 day can be safely retracted in favour of its neighbour at 2.65 day (significance 2.4σ). The period value of 1.6 day is also rather unlikely, albeit now $\mathcal{V} \approx 1.8$, which is only moderately significant.

6.5 Exoplanetary system orbiting HD156668

On the basis of the Keck observations, Howard et al. (2011) reported that this star is orbited by a super-Earth having short period of 4.6 days or, possibly, 1.2 days. As Dawson & Fabrycky (2010) claim, the correct value of the period should be 1.2 days, and the peak at 4.6 day is only its diurnal alias. Let us try to verify these results too. First, we can see that there are actually more than two possible periods at stack (Fig. 8, top). For further investigation we select four periodogram peaks for periods longer than half-day. We

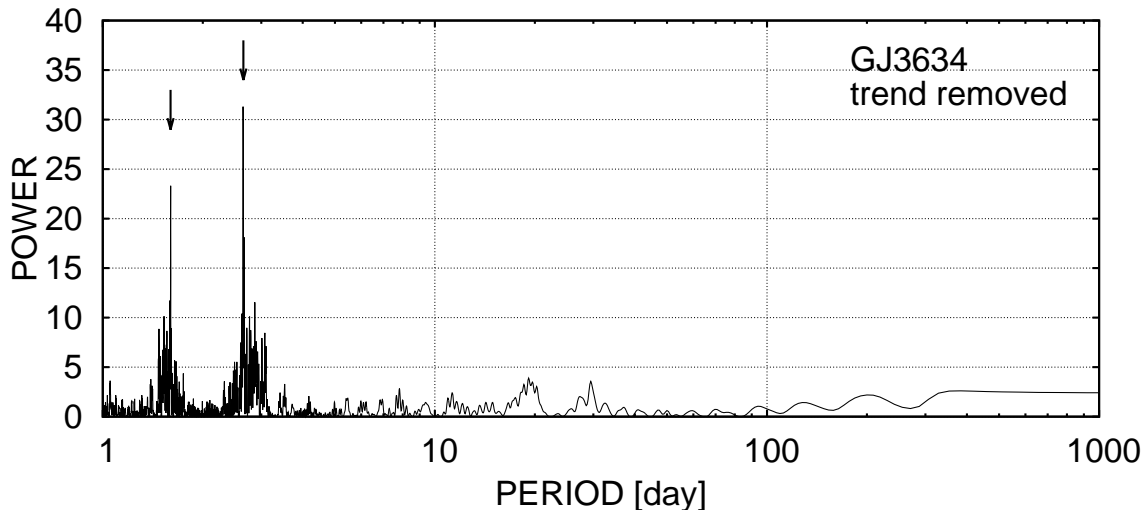


Figure 7. Residual periodogram of GJ3634 radial velocities, with long-term quadratic drift removed. We can see two peaks here. The peak at 2.6 days is actually double. The Vuong test suggests to select the higher peak at 2.6 day in comparison with the peak at 1.6 day, but at a moderate significance of 1.8σ . The smaller peak near 2.6 day can be rejected at 2.4σ .

Table 2. Comparing four alias alternatives for HD156668 *b*: values of \mathcal{V} obtained for various alias pairs

Alias	4.6 d	0.56 d	800 d
1.2 d	0.9	0.8	0.5
4.6 d	—	0.3	0.2
0.56 d	—	—	0.0

fit four corresponding models assuming circular orbit⁵ and calculate the Vuong statistic for each pair of these models. The results are given in Table 2. Investigating this table, we can see that the Vuong statistic is always small (< 1). Thus our results do not support the conclusion made by Dawson & Fabrycky (2010) concerning this planet.

We prefer to remain cautious also because it seems that some extra variations may be present in the radial velocity of this star. The residual periodogram with, say, 1.2-day oscillation subtracted off, demonstrates that the peak at 800 days does *not* disappear (Fig. 8, bottom). Its height (and thus significance) appears the same as for the first period that we extracted. Indeed, using the methods described in (Baluev 2008, 2009) we find that this peak infers the false alarm probability of only 0.1%. It does not matter if we try to extract first the periodicity of 4.6 day or 0.56 day instead of 1.2 day, the 800-day peak remains here. On contrary, extracting this 800-day peak at the first place does not eliminate the three remaining peaks at short periods. Speaking shortly, three short periods are mutual aliases of each other, while 800-day period is a standalone entity.

This long-period variation might represent a hint of an extra planet, or maybe of some other phenomenon, like the red noise effect in the RV data for GJ876 (Baluev 2011).

⁵ The orbital eccentricity looks ill-determined in this case, because it often rises to unrealistic values. Also, due to the famous tidal orbit circularization effect, it is unlikely that an eccentric orbit could reside so close to the star.

Indeed, similarly to the GJ876 case, we can see in this periodogram a broad band of low-frequency peaks without any standalone clearly dominating peak (either 800 days or any other). Just like any usual harmonic periodicity, this low-frequency band produces a diurnal alias band around the period of 1 day. This diurnal band is actually clearly seen in the periodogram, and it might easily enforce the 1.2-day peak, relatively to the 4.6-day one. This argumentation, along with a small value of the Vuong statistic, forces us to disobey the recommendation by Dawson & Fabrycky (2010) to leave only 1.2 day period as the correct solution. We do not find a rigorous statistical basis for this in the current data.

7 CONCLUSIONS AND DISCUSSION

We have introduced the Vuong test, which is an asymptotically normal statistical test for verifying the observational equivalence of alternative models. This method compares the alternative models in the sense of certain statistical measure of their divergence. The Vuong statistic uses the Kullback-Leibler Information Criterion to establish whether the models are equivalent or not. Importantly, this test does not require that one of the rival models should be correct. Instead, both alternatives may occur formally wrong (misspecified case). Such models are still correctly ordered in terms of the adopted divergence measure. We classify this as a high practical advantage, since in practice no model is precisely correct: any data always contain some hidden residual variations and the true error distribution may deviate from the normal function. We should however admit that any ordering of the alternatives is not very useful if all available alternatives are too far from the truth. Another important advantage of our test is due to its practical simplicity and calculation speed. It is fully analytic and does not require any CPU-consuming simulations in the routine use.

Throughout the paper, we mainly focused our attention on the period ambiguity issue, since this is one of the most

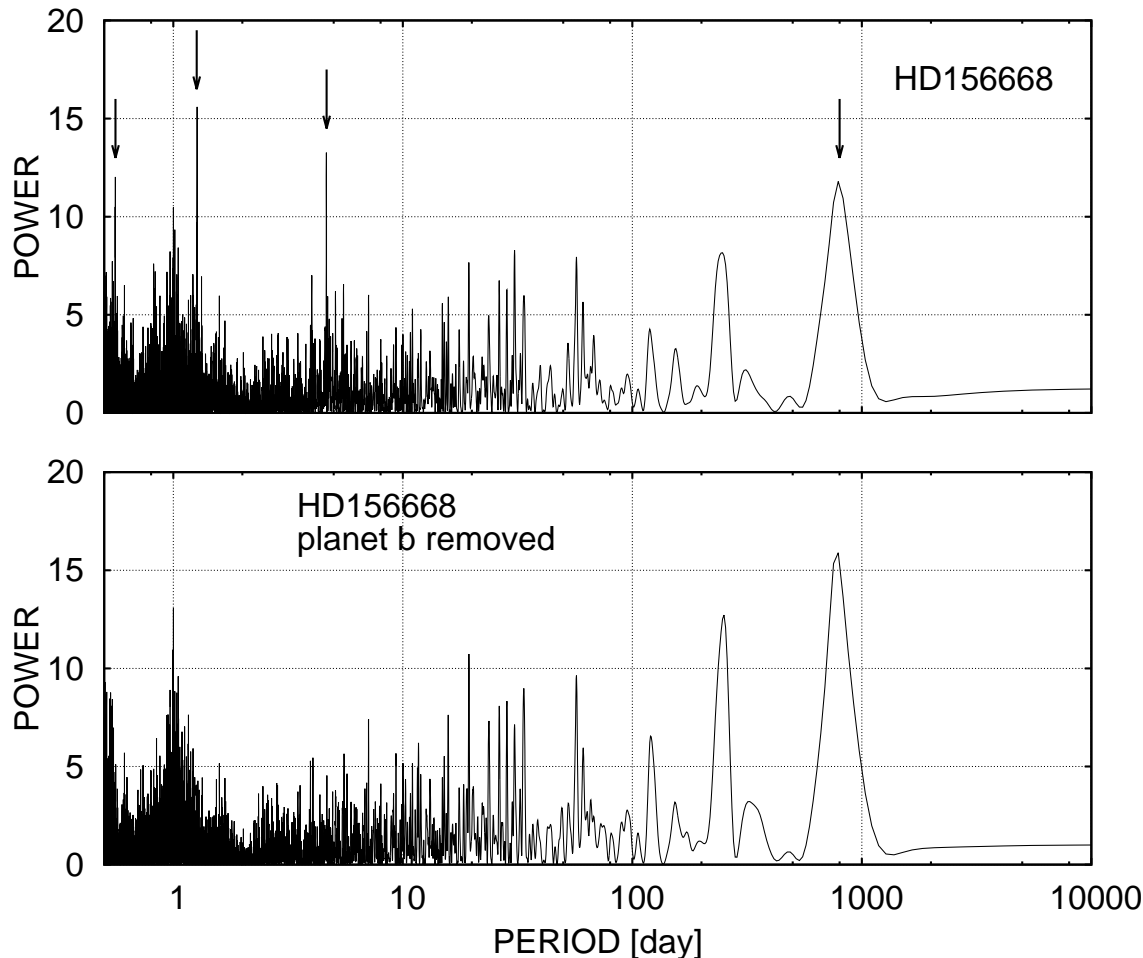


Figure 8. Top: periodogram of HD156668 radial velocity data calculated according to (Baluev 2009) and involving only a constant term in the base model. Bottom: similar residual periodogram with planet b sinusoidal signature embedded in the base model as well (and assuming the period $P_b \approx 1.2$ days). In the second periodogram, the peak at 800 days remains intact (and even enforced). It has the same significance as the 1.2-day peak in the first periodogram. Here we disagree with Dawson & Fabrycky (2010), who suggested the 1.2 days peak as a definite solution.

practical task. However, the Vuong test can be also applied to check the model equivalence in other situations, when the ambiguity is related to any other parameters (not necessarily the period). The main necessary formulae of the test remain basically the same.

We have reanalysed the radial velocity data for several extrasolar planetary systems. We verified that orbital periods of the planets 55 Cnc e , HD75898 b and GJ876 d can be resolved unambiguously on the basis of presently available data, while the period of HD156668 b and the eccentricity of the planet GJ876 e are still ambiguous.

A popular rival approach for solving such disambiguation tasks is the Bayesian model selection (e.g. Gregory 2007). However, the great disadvantage of the Bayesian methods is their computational complexity requesting for intensive numerical simulations. The Vuong test is completely free from this disadvantage. Also, when dealing with a task like distinguishing between different alternatives, we should always have an adequate impression of which statement is derived from the real observations, and which one follows from an a priori assumption not tied to the actually ob-

served data. This impression is difficult to obtain if we use Bayesian statistics, especially when we compare two solutions from very different regions of the parameter space. Basically, Bayesian methods mix the subjective prior assumptions with the objective information derived from the real data, which makes them, in our view, often unsuitable for model intercomparison. We do not decline the known strengths of the Bayesian methods, but we must mention that debates on the Bayesianism still do not cease (Efron 1986; Gelman 2008). In practice, it is always necessary to verify that the results of the Bayesian analysis are stable with respect to choosing different reasonable prior distributions. If this stability is not ensured, then there is a risk that such analysis is in fact more based on the prior assumptions rather than on the real data.

The Vuong test is not Bayesian, but it does not implicitly assume any specific prior distributions. Although subjective assumptions are never purged out completely, we can pursue to minimize their influence. The Vuong test attains good resistance to this undesired influence. We count it as its great advantage.

ACKNOWLEDGMENTS

This work was supported by the Russian Academy of Sciences research programme “Non-stationary phenomena in the objects of the Universe”. I am grateful to the reviewers for their insightful comments on this manuscript.

REFERENCES

- Baluev R. V., 2008, *MNRAS*, 385, 1279
 Baluev R. V., 2009, *MNRAS*, 393, 969
 Baluev R. V., 2011, *Celest. Mech. Dyn. Astron.*, 111, 235
 Bonfils X., Gillon M., Forveille T., Delfosse X., Deming D., Demory B.-O., Lovis C., Mayor M., Neves V., Perrier C., Santos N. C., Seager S., Udry S., Boisse I., Bonnetfoy M., 2011, *A&A*, 528, A111
 Correia A. C. M., Couetdic J., Laskar J., Bonfils X., Mayor M., Bertaux J.-L., Bouchy F., Delfosse X., Forveille T., Lovis C., Pepe F., Perrier C., Queloz D., Udry S., 2010, *AA*, 511, A21
 Cox D. R., 1962, *J. Roy. Stat. Soc. B*, 24, 406
 Dawson R. I., Fabrycky D. C., 2010, *ApJ*, 722, 937
 Efron B., 1986, *American Statistician*, 40, 1
 Fischer D. A., Marcy G. W., Butler R. P., Vogt S. S., Laughlin G., Henry G. W., Abouav D., Peek K. M. G., Wright J. T., Johnson J. A., McCarthy C., Isaacson H., 2008, *ApJ*, 675, 790
 Frescura F. A. M., Engelbrecht C. A., Frank B. S., 2008, *MNRAS*, 388, 1693
 Gelman A., 2008, *Bayesian Analysis*, 3, 445
 Gourieroux C., Monfort A., Trognon A., 1984, *Econometrica*, 52, 681
 Goździewski K., Breiter S., Borczyk W., 2008, *MNRAS*, 383, 989
 Goździewski K., Konacki M., Maciejewski A. J., 2006, *ApJ*, 645, 688
 Goździewski K., Maciejewski A. J., Migaszewski C., 2007, *ApJ*, 657, 546
 Gregory P. C., 2005, in Knuth K. H., Abbas A. E., Morris R. D., Castle J. P., eds, *Bayesian Inference and Maximum Entropy Methods*. Vol. 803 of *AIP Conf. Proc.*, A Bayesian analysis of extrasolar planet data for HD208487. *Am. Inst. Phys.*, New York, pp 139–145
 Gregory P. C., 2007, *MNRAS*, 374, 1321
 Howard A. W., Johnson J. A., Marcy G. W., Fischer D. A., Wright J. T., Henry G. W., Isaacson H., Valenti J. A., Anderson J., Piskunov N. E., 2011, *ApJ*, 726, 73
 Lomb N. R., 1976, *Ap&SS*, 39, 447
 Rivera E. J., Laughlin G., Butler R., Vogt S., Haghighipour N., Meschiari S., 2010, *ApJ*, 719, 890
 Robinson S. E., Laughlin G., Vogt S. S., Fischer D. A., Butler R. P., Marcy G. W., Henry G. W., Driscoll P., Takeda G., Johnson J. A., 2007, *ApJ*, 670, 1391
 Scargle J. D., 1982, *ApJ*, 263, 835
 Vityazev V. V., 2001, *Analysis of Uneven Time Series*. SPb Univ. Press, Saint Petersburg
 Vogt S. S., Butler R. P., Marcy G. W., Fischer D. A., Henry G. W., Laughlin G., Wright J. T., A. J. J., 2005, *ApJ*, 632, 638
 Vuong Q. H., 1989, *Econometrica*, 57, 307
 Zechmeister M., Kürster M., 2009, *A&A*, 496, 577

APPENDIX A: MEANING OF THE RANDOM TIMINGS

It is an essential peculiarity of the Vuong test that it treats the timings and measurement uncertainties as random quantities. This randomness is not related to possible inaccuracies in the determined values of t_i and σ_i . Instead, it is related to the observations scheduling, which is treated as a random process. This issue should be clarified in more details now.

In the astronomical practice, it is rarely taken into account that the time of an observation is often a random quantity, broadly analogous to the random measurement error. It is usually assumed that t_i (as well as σ_i) are fixed a priori for each data set analysed. It is assumed that all statistical uncertainties in any data-derived quantities are caused only by random errors in x_i . Basically, we implicitly embed the observed data set into a general ensemble of hypothetical similar time series, each having its own sequence of x_i and still the same sequence of t_i . This restrictive assumption about t_i may have undesired effect sometimes. To demonstrate this, assume that we are carrying out a large survey of many astronomical targets. In practice, the timings of individual observations are always distributed according to some observational time window, which often shows some regular patterns (e.g. periodic gaps), but within this time window they are usually distributed pretty randomly. Usually we cannot take a snapshot of all targets at once, so each target has individual time series with different sequence of t_i . Under such circumstances, the random scatter of any data-derived quantity (e.g., some parametric estimation or a test statistic) incorporates an extra contribution inferred by the random fluctuations of t_i . When we subsequently apply our statistical procedure to each target of such survey, we should encounter, in general, more blurred uncertainties and more frequent false alarms than we can expect assuming that all t_i are fixed. Therefore, to deal with this situation properly, we should consider another general ensemble of time series, which admits of random variations in t_i and σ_i , as well as in x_i .

We do not try to scare the reader by claiming that all results of any data analysis done so far should be now rechecked taking into account the possible fluctuations of t_i . The quantities used traditionally in the astronomical data analysis, are often statistically invariable with respect to the exact sequence of t_i . “Statistically invariable” means here that the corresponding distribution function is invariable with respect to fluctuations of t_i within any given distribution pattern, although individual values of the test statistic usually do depend on t_i . For example:

(i) It is well-known that the values of the Lomb-Scargle periodogram are exponentially distributed, regardless the actual sequence of timings. Consequently, they remain exponentially distributed for the random t_i too.

(ii) According to Baluev (2008), the tail distribution of the maximum peaks of the Lomb-Scargle periodogram can be approximated by a formula $We^{-z}\sqrt{z}$, where W is proportional to the sample variance of t_i . For large N , the latter variance is practically invariable with respect to random fluctuations of t_i , if these fluctuations obey some well-specified time window. Therefore, the distribution of the

maximum periodogram peaks also should not be significantly affected by the fluctuating timings.

(iii) The maximum-likelihood (or least-square) estimations of various model parameters are usually asymptotically unbiased for large N , with the uncertainty approximately proportional to $1/\sqrt{N}$. The distribution of such estimations is asymptotically invariable with respect to the random variations of t_i , if these variations follow any specified time window. The uncertainties of the estimations may often depend on this time window, however.

When t_i (and σ_i) are treated as fixed non-random quantities, the distribution of the Vuong statistic significantly depends on their exact sequence. This can be easily demonstrated. We can avoid dealing with any distribution of t_i if we redefine the KLIC divergence as

$$\begin{aligned} \text{KLIC}'_{12}(\boldsymbol{\theta}_1, \boldsymbol{\theta}_2, \mathbf{z}) &= \frac{1}{N} \mathbb{E}_{\mathbf{x}|\mathbf{z}}^0 \sum_{i=1}^N \log \frac{f_1(x_i|z_i, \boldsymbol{\theta}_1)}{f_2(x_i|z_i, \boldsymbol{\theta}_2)} = \\ &= \frac{1}{N} \mathbb{E}_{\mathbf{x}|\mathbf{z}}^0 \log \frac{\mathcal{L}_1(\mathbf{x}|\mathbf{z}, \boldsymbol{\theta}_1)}{\mathcal{L}_2(\mathbf{x}|\mathbf{z}, \boldsymbol{\theta}_2)}, \end{aligned} \quad (\text{A1})$$

where the expression under the \mathbb{E}^0 sign represents now the usual (observed) log-likelihood ratio for the two models, and the expectation itself is now taken conditionally to fixed z_i . This new divergence measure represents a direct analog of the quantity (4), but calculated for a particular discrete sequence of z_i . There is no obstacle to use the same Vuong statistic (7) to test the new null hypothesis $\text{KLIC}'_{12} = 0$, which is apparently no worse than testing the hypothesis $\text{KLIC}_{12} = 0$. Indeed, the value of KLIC'_{12} , which represents an average over the N timings, should converge to KLIC_{12} for $N \rightarrow \infty$. Since we anyway consider only this asymptotic case, the two measures KLIC and KLIC' are just equivalent, and the quantity L in (5) can be used to estimate both. However, the variance of L is misbehaving: it has systematically different values for fixed z_i and for random z_i . This occurs because random fluctuations in x_i and in z_i generate comparable contributions in the total variance of L . Thus the mentioned variance should be significantly smaller for fixed z_i than for random z_i .

It is not hard to show this rigorously. Indeed, when z_i are treated random, all l_i have the same distribution, and it is easy to derive that

$$\mathbb{E}_{\mathbf{x}, \mathbf{z}}^0 v^2 \simeq \mathbb{D}_{\mathbf{x}, \mathbf{z}}^0 l, \quad \mathbb{E}_{\mathbf{x}, \mathbf{z}}^0 L = \mathbb{E}_{\mathbf{x}, \mathbf{z}}^0 l, \quad N \mathbb{D}_{\mathbf{x}, \mathbf{z}}^0 L = \mathbb{D}_{\mathbf{x}, \mathbf{z}}^0 l, \quad (\text{A2})$$

where \mathbb{D} stands for the variance operator, $\mathbb{D}x = \mathbb{E}x^2 - (\mathbb{E}x)^2$. We can see that in this case the normalised statistic $\mathcal{V} = L\sqrt{N}/v$ indeed should approximately follow the standard normal distribution. When z_i are fixed, the averaging over z_i in (A1) and any derived formulae can approximate the expectation $\mathbb{E}_{\mathbf{z}}$. Applying this rule, we may derive

$$\mathbb{E}_{\mathbf{x}|\mathbf{z}}^0 v^2 \simeq \mathbb{D}_{\mathbf{x}, \mathbf{z}}^0 l, \quad \mathbb{E}_{\mathbf{x}|\mathbf{z}}^0 L \simeq \mathbb{E}_{\mathbf{x}, \mathbf{z}}^0 l, \quad N \mathbb{D}_{\mathbf{x}|\mathbf{z}}^0 L \simeq \mathbb{E}_{\mathbf{z}}^0 \mathbb{D}_{\mathbf{x}|\mathbf{z}}^0 l. \quad (\text{A3})$$

We can see that v^2 did not attain any significant systematic bias, as well as L , while the variance of L is now different:

$$\begin{aligned} N (\mathbb{D}_{\mathbf{x}, \mathbf{z}}^0 - \mathbb{D}_{\mathbf{x}|\mathbf{z}}^0) L &\simeq \mathbb{D}_{\mathbf{x}, \mathbf{z}}^0 l - \mathbb{E}_{\mathbf{z}}^0 \mathbb{D}_{\mathbf{x}|\mathbf{z}}^0 l = \\ &= \mathbb{E}_{\mathbf{z}}^0 (\mathbb{E}_{\mathbf{x}|\mathbf{z}}^0 l)^2 - (\mathbb{E}_{\mathbf{z}}^0 \mathbb{E}_{\mathbf{x}|\mathbf{z}}^0 l)^2 = \mathbb{D}_{\mathbf{z}}^0 \mathbb{E}_{\mathbf{x}|\mathbf{z}}^0 l \geq 0. \end{aligned} \quad (\text{A4})$$

Therefore, if we consider our situation conditionally to fixed z_i , we find that the variance of the Vuong statistic is systematically smaller than unit. This variance deficit does

not tend to zero when $N \rightarrow \infty$. Instead, it stabilizes at a constant value $\mathbb{D}_{\mathbf{z}}^0 \mathbb{E}_{\mathbf{x}|\mathbf{z}}^0 l / \mathbb{D}_{\mathbf{x}, \mathbf{z}}^0 l$. It is difficult to apply the Vuong test in such situation, since then the exact variance of \mathcal{V} is unknown even for $N \rightarrow \infty$, although we know that it cannot exceed unit. The variance deficit of \mathcal{V} disappears only in a very specific case when $\mathbb{E}_{\mathbf{x}|\mathbf{z}}^0 l$ is constant in z .

However, we must emphasize again that the Vuong test does not request to specify the distribution of t_i and σ_i explicitly. In practice, we should not care about this distribution at all, and the practical application of the test is easy. In other words, although the Vuong test is sensitive to the presence of random fluctuations of individual timings, it is invariable with respect to their *distribution* reflecting the shape of the time window.

We still can imagine practical cases falling out of the random interpretation of the timings. For example, when we take a sequence of images of the same field, it makes the timings non-random – they appear always the same for all targets of such fixed-field survey. In this case, however, the Vuong test does not stop working. As we have just shown, the variance of the Vuong statistic can only decrease when we move from random t_i to fixed t_i , so when we apply it to such fixed-field survey, we still obtain at least an upper limit on the false alarm probability. This means that if the Vuong test recommends to retract the null (equivalence) hypothesis at e.g. 99% level, we can safely retract it even if the sampling patterns are the same for all our targets: the true confidence level maybe possibly larger than 99%, but this only implies even larger significance. The only negative consequence is that in the case of so specific data sampling we can distinguish more close alternatives than usually, and the Vuong test does not catch this opportunity. That is, another test having better sensitivity in this specific situation may exist, but it is hardly as general as the Vuong one.

This paper has been typeset from a $\text{T}_{\text{E}}\text{X}/\text{L}^{\text{A}}\text{T}_{\text{E}}\text{X}$ file prepared by the author.